Model predictive temperature control for a food transporter with door-openings

Elisabeth Luchini[1†], Agnes Poks[1], Dominik Radler[2] and Martin Kozek[1]

[1]Institute of Mechanics and Mechatronics Division of Control and Process Automation, Getreidemarkt 9/325-A5, A-1060 Vienna, Austria
(Tel: +43-1-58801-325527; E-mail: elisabeth.luchini@tuwien.ac.at)
[2]PRODUCTBLOKS GmbH, Stockerauer Str. 106, 2100 Korneuburg, Austria

Abstract: Temperature control of a food supplier vehicle with an insulated cool box (ICB) is critical. Air exchange during the door-opening is a main disturbance which heats up the ICB and accounts for a large part of total cooling load. Usually, this effect is not considered in the control strategy. In this paper a model predictive control (MPC) is used to optimise the temperature control and energy consumption and to handle the door-opening effects. Due to the thermal inertia of the cargo, it can be shown that a technique for estimating the temperature of the cargo instead of the air temperature would lead to a more effective control system. The system and control architecture is presented, the concept of the MPC including door-opening is given and simulation results demonstrate the performance of the concept.

Keywords: model predictive control, door-opening, air exchange, refrigeration system

1. INTRODUCTION

Food transport systems are widely used. There are at least one million refrigerated road vehicles in use in the world, [1]. Every day food transporters deliver valuable goods to supermarkets and pharmacies. Therefore, one of the objectives of technical development is to increase their energy efficiency and to avoid wasted food due to cooling temperature violations.

The main target for the refrigeration in road vehicles is to hold the desired set temperature of the insulated cool box (ICB) in order to prevent degeneration of perishable goods. At the same time a minimisation of the energy consumption of the refrigeration system is desired. Model predictive control (MPC) is an attractive method for such a system where conflicting targets and predictions of disturbances such as ambient temperature and solar radiation exist. Furthermore, operational and technological constraints can be easily incorporated in the optimisation strategy. In [2] a MPC for redundant refrigeration circuits (RCs) is presented. To deal with the hybrid nature of the refrigeration systems a hierarchical control concept is used. The MPC optimises the temperature of the ICB, while a mixed-integer MPC provides the actual cooling capacity. The stability of such a system is demonstrated in [3]. Solar irradiation, ageing effects of the ICB and door-opening disturb the optimal control of the MPC and act as unknown input. There are methods to estimate such disturbances. In [4] and [5] the solar irradiation and ageing effect of a transporter are explained. An observer is used for estimating the heat flow based on the disturbances. With an ageing model the heat flow can be separated into the part which comes from the solar irradiation and the part which comes from the ageing of the ICB.

Infiltration of warm ambient air through door-opening accounts for a large part of total cooling load. Infiltration through the doorway of cold stores is responsible for more than half of the total cooling load [6]. Therefore, many researches have carried out experiments and simulation studies on the characteristics and predictions of the infiltration airflow. In [7] the prediction performance of a series of steady models and a transient CFD model against the experimental results of a refrigerated room is compared. [8] deals with an experimental and numerical investigation of heat and mass infiltration rates during the opening of a refrigerated truck body. In [9] a transient infiltration simulation model is established. The model is validated by the experimental data of a cold store under conditions with different temperature differences, opening sizes of the door and operation mode of the cooling fans. In order to find a simple and accurate method to measure the transient infiltration airflow rates through the doorway of cold stores, a method based on the local air velocity linear fitting is proposed in [10]. In [11] has been proposed an unsteady analytical model for predicting the transient infiltration airflow rate into refrigerated spaces, based on the time-dependent differential equations of motion and continuity. The analytical model was successfully validated with experiments.

In the state of the art the ICB temperature which is defined by the air temperature of the ICB is used as the control variable, which is a very simple and cost-effective way. Nevertheless, caused by the small mass and thermal capacity of the air this temperature is critical compared to the real temperature of the cargo. Especially the door-opening has a high impact on the air temperature. In this paper it can be seen that this leads to an immense cooling effort although the goods are not effected.

The remainder of the paper is structured as follows: In Section 2 the model of the ICB and the refrigeration system including the door-opening are presented. An overview of the control structure, the structure of the MPC and the constraints is made in Section 3. Simulation results are shown in Section 4. A short discussion and conclusion finalises the paper.

† Elisabeth Luchini is the presenter of this paper.

20SY0003/0000-1314© 2020 SICE

2. SYSTEM DESCRIPTION

2.1. Insulated cool box model

The insulation of the ICB consists of an outer and inner steel layer with several polyurethane (PU) foam layers. The temperature of the outside and inside steel layer is defined by $\vartheta_{\text{steel,out}}$ and $\vartheta_{\text{steel,in}}$. The different PU foam layers are defined by $\vartheta_{\text{PU,i}}$, where $i = 1 \dots n_{pu}$ is the index of the PU layer and n_{pu} the number of PU layers, see Fig. 1.

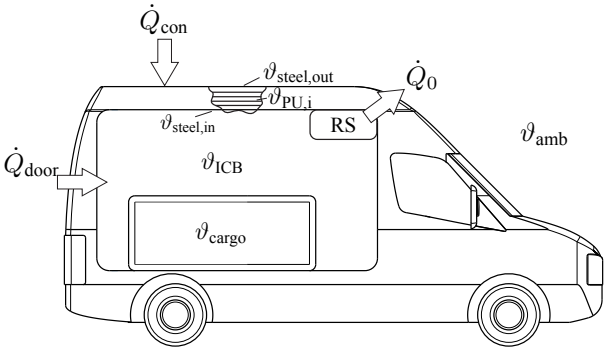

Fig. 1 Model of the insulated cool box.

The door-opening $\dot{Q}_{\text{door}}$ and the cooling capacity $\dot{Q}_0$ act directly on ϑ_{ICB}, the ambient temperature ϑ_{amb} affects only the outer steel layer:

$$\dot{Q}_{\text{con}} = \alpha_n A_{\text{iso}}(\vartheta_{\text{amb}} - \vartheta_{\text{steel,out}}), \tag{1}$$

where α_n is the heat transfer coefficient of the outside steel layer and A_{iso} the insulation surface of the ICB.

The temperature change of all temperatures can be described by the coupled linear differential equations

$$\begin{aligned}
m_1 c_{p,1} \dot{\vartheta}_{\text{cargo}} &= \alpha_1 A_{\text{cargo}}(\vartheta_{\text{ICB}} - \vartheta_{\text{cargo}}) && (2)\\
m_2 c_{p,2} \dot{\vartheta}_{\text{ICB}} &= -\alpha_1 A_{\text{cargo}}(\vartheta_{\text{ICB}} - \vartheta_{\text{cargo}}) \\
&+ \alpha_2 A_{\text{iso}}(\vartheta_{\text{steel,in}} - \vartheta_{\text{ICB}}) \\
&+ \dot{Q}_0 + \dot{Q}_{\text{door}} && (3)\\
m_3 c_{p,3} \dot{\vartheta}_{\text{steel,in}} &= -\alpha_2 A_{\text{iso}}(\vartheta_{\text{steel,in}} - \vartheta_{\text{ICB}}) \\
&+ \alpha_3 A_{\text{iso}}(\vartheta_{\text{PU,1}} - \vartheta_{\text{steel,in}}) && (4)\\
m_{(3+i)} c_{p,(3+i)} \dot{\vartheta}_{\text{PU,i}} &= -\alpha_{(3+i-1)} A_{\text{iso}}(\vartheta_{\text{PU,i}} - \vartheta_{\text{PU,i-1}}) \\
&+ \alpha_{(3+i)} A_{\text{iso}}(\vartheta_{\text{PU,i+1}} - \vartheta_{\text{PU,i}}) && (5)\\
m_n c_{p,n} \dot{\vartheta}_{\text{steel,out}} &= -\alpha_{(n-1)} A_{\text{iso}}(\vartheta_{\text{steel,out}} - \vartheta_{\text{PU,n}_{\text{pu}}}) \\
&+ \dot{Q}_{\text{con}}, && (6)
\end{aligned}$$

where m_i describes the masses, $c_{p,i}$ the thermal capacities, α_i the heat transfer coefficient and A_{cargo} the surface of the cargo. The number of equations depends on the different layers of the PU foam layers n_{pu} and is defined as $n = 4 + n_{\text{pu}}$.

The plant output is the ICB temperature ϑ_{ICB}, the control variable is given by the cooling capacity $\dot{Q}_0$, and ϑ_{amb} and $\dot{Q}_{\text{door}}$ are the main disturbances. Typically, only sensor signals for ϑ_{ICB} and ϑ_{amb} are available.

A simplified temperature model where additional irradiation from the sun and a time-varying heat transfer coefficient is included can be found in [5].

2.2. Refrigeration system

The refrigeration system (RS) consists of a refrigeration circuit (RC) which includes a condenser, an evaporator, an electronic expansion valve and a compressor, see Fig. 2.

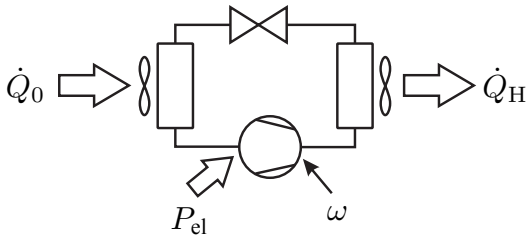

Fig. 2 Structure of the RS, with the electrical power P_{el}, the rotational speed ω and the heat flow $\dot{Q}_H$ which is delivered to the environment.

The RS is modelled by nonlinear static relations $f_i(\omega, \vartheta_{\text{amb}}, \vartheta_{\text{ICB}})$. The cooling capacity u_0 and electrical power consumption P_{el} are the outputs of these static relations. Dynamic behaviour of the RS is neglected, such dynamics can be found in [2]. The real vapour compression cycle is in fact complex and not fully state controllable, [12, 13]. Here it is assumed that the static nonlinearities f_i contain optimal operating points for the vapour compression cycle, and that remaining inner states are regulated by dedicated control loops (e.g. superheat temperature).

2.3. Door-opening model

During a door-opening part of the air in the ICB is exchanged with air at ambient temperature. To predict the heat input during a door-opening the results of [8] are used. In this paper experiments on the infiltration heat load during door-opening of a refrigerated truck are presented. The data are adapted to the dimension of the ICB and can be seen in Fig. 3.

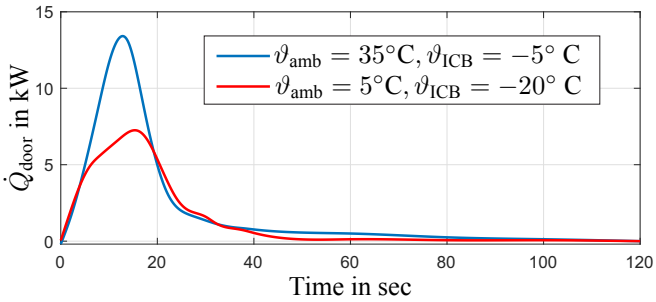

Fig. 3 Heat flow during door-opening for different conditions.

With the assumption that a door only opens during a good withdrawal, the mass of the goods also decreases with each door-opening. The cargo mass which is unloaded from the ICB is defined by d_{cargo}. The information of vehicle position and unloading locations is already available today. Therefore, the MPC can react before the door-opening happens and the negative effect of the door-opening can be minimised.

3. CONTROL STRATEGY

3.1. Control structure

In Fig. 4 the control strategy can be seen. The linear MPC uses the reference ICB temperature $\vartheta_{\text{ICB}}^{\text{ref}}$, which is typically constant, and the trajectories for the ambient temperature $\boldsymbol{\vartheta}_{\text{amb}}^{\text{traj}}$ and the door-opening $\dot{\boldsymbol{Q}}_{\text{door}}^{\text{traj}}$. It is assumed that both trajectories are known from predictions. Weather data is easily available from weather forecasts and $\dot{\boldsymbol{Q}}_{\text{door}}^{\text{traj}}$ depends on Fig. 3 and the defined route of the vehicle.

The MPC computes the optimal cooling capacity $\dot{Q}_0^{\star}$ which is transformed into the compressor speed ω using the static maps of the RS together with the measured ambient temperature. The actual cooling capacity $\dot{Q}_0$ of the RS is then applied to the ICB.

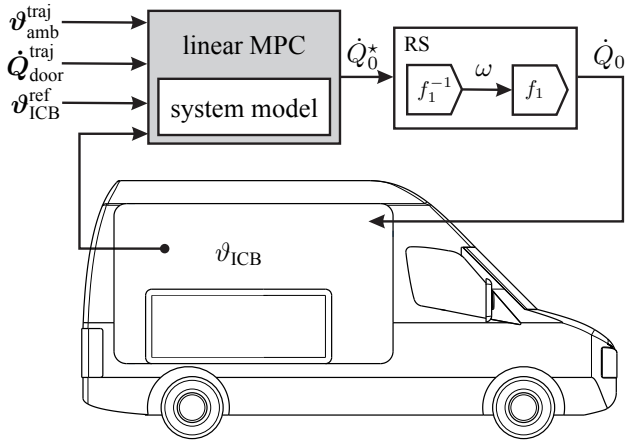

Fig. 4 Control structure with the MPC and the RS.

3.2. Control method

3.2.1. MPC formulation

Standard MPC formulations are well-known and given e.g. in [14]. The state vector $\boldsymbol{x}$ is defined by

$$\boldsymbol{x} = \begin{bmatrix} \vartheta_{\text{cargo}} \\ \vartheta_{\text{ICB}} \\ \vartheta_{\text{steel,in}} \\ \vartheta_{\text{PU,1}} \\ \vdots \\ \vartheta_{\text{PU,i}} \\ \vdots \\ \vartheta_{\text{PU,n}_{\text{pu}}} \\ \vartheta_{\text{steel,out}} \end{bmatrix} \in \mathbb{R}^{(n \times 1)}. \tag{7}$$

The dynamic ICB model, eqns. (2)-(6), is discretised with a zero order hold method and a sample time of T_s. The discretised linear state-space model is formulated as:

$$\begin{aligned} \boldsymbol{x}(k+1) &= \boldsymbol{A}\boldsymbol{x}(k) + Bu(k) + \boldsymbol{E}\boldsymbol{z}(k) && (8) \\ y(k) &= \boldsymbol{C}\boldsymbol{x}(k), && (9) \end{aligned}$$

with k the sampling instance of the MPC, the system matrix $\boldsymbol{A} \in \mathbb{R}^{(n \times n)}$, input matrix $\boldsymbol{B} \in \mathbb{R}^{(n \times 1)}$, output matrix $\boldsymbol{C} \in \mathbb{R}^{(1 \times n)}$ and disturbance matrix $\boldsymbol{E} \in \mathbb{R}^{(n \times 2)}$ and

$$\begin{aligned} u(k) &= \dot{Q}_0(k) \in \mathbb{R}^{(1 \times 1)}, \\ z(k) &= \begin{bmatrix} \vartheta_{\text{amb}}(k) & \dot{Q}_{\text{door}}(k) \end{bmatrix}^T \in \mathbb{R}^{(2 \times 1)}. \end{aligned}$$

3.2.2. Prediction of state and output variables

Based on the state-space model the future state variables are calculated sequentially using the set of future control inputs

$$\boldsymbol{U}(k) = \begin{bmatrix} U(k) \\ U(k+1) \\ \vdots \\ U(k+N_{\text{c}}-1) \end{bmatrix},$$

where N_{c} is the control horizon of the MPC. The prediction is given by

$$\hat{\boldsymbol{Y}}(k) = \boldsymbol{F}\hat{\boldsymbol{x}}(k) + \boldsymbol{\Phi}_u \boldsymbol{U}(k) + \boldsymbol{\Phi}_z \boldsymbol{Z}(k), \tag{10}$$

where the matrices $\boldsymbol{F}, \boldsymbol{\Phi}_u$ and $\boldsymbol{\Phi}_z$ are computed as described in [15] and

$$\hat{\boldsymbol{Y}}(k) = \begin{bmatrix} \hat{y}(k+1|k) \\ \hat{y}(k+2|k) \\ \vdots \\ \hat{y}(k+N_{\text{p}}|k) \end{bmatrix}$$

is the predicted output, where N_{p} is the prediction horizon of the MPC and

$$\boldsymbol{Z}(k) = \begin{bmatrix} \boldsymbol{Z}(k|k) \\ \boldsymbol{Z}(k+1|k) \\ \vdots \\ \boldsymbol{Z}(k+N_{\text{p}}-1|k) \end{bmatrix}^T$$

includes the disturbance trajectories for $\boldsymbol{\vartheta}_{\text{amb}}^{\text{traj}}$ and $\dot{\boldsymbol{Q}}_{\text{door}}^{\text{traj}}$.

The reference trajectory $\boldsymbol{Y}_{\text{ref}}(k)$ is defined as

$$\boldsymbol{Y}_{\text{ref}}(k) = \begin{bmatrix} \vartheta_{\text{ICB}}^{\text{ref}}(k+1) \\ \vartheta_{\text{ICB}}^{\text{ref}}(k+2) \\ \vdots \\ \vartheta_{\text{ICB}}^{\text{ref}}(k+N_{\text{P}}) \end{bmatrix}.$$

3.2.3. Constraints

Due to the physical hard constraints on the RS, constraints to the control variable have to be defined:

$$\boldsymbol{U}_{\text{min}}(k) \leq \boldsymbol{U}(k) \leq \boldsymbol{U}_{\text{max}}(k), \tag{11}$$

where $\boldsymbol{U}_{\text{min}}$ and $\boldsymbol{U}_{\text{max}}$ are the time-variant maximal and minimal available cooling capacity of the RS.

To enforce the reference temperature of the ICB a slack variable is defined:

$$\boldsymbol{s}(k) = \boldsymbol{Y}_{\text{ref}}(k) - \hat{\boldsymbol{Y}}(k), \tag{12}$$

where $\boldsymbol{s}$ define the soft constraint on the output. Therefore, a deviation of the temperature is allowed, but will be penalised. This is used to define the allowed region of the ICB temperature. If $\vartheta_{\text{ICB}}^{\text{ref}}$ is positive the temperature of the ICB should always be greater than $0°\text{C}$ to avoid freezing, if $\vartheta_{\text{ICB}}^{\text{ref}}$ is negative the temperature of the ICB should always be smaller than $0°\text{C}$ to avoid unfreezing.

3.2.4. Optimisation

To enforce the reference temperature of the ICB and ensure feasibility for all conditions the optimisation criterion with input constraints is chosen as

$$\begin{aligned} J &= \boldsymbol{U}^T(k)\boldsymbol{R}_1\boldsymbol{U}(k) + \boldsymbol{s}^T(k)\boldsymbol{R}_2\boldsymbol{s}(k) \\ &\text{s.t.} \\ &\boldsymbol{U}_{\min}(k) \leq \boldsymbol{U}(k) \leq \boldsymbol{U}_{\max}(k), \end{aligned} \tag{13}$$

where $\boldsymbol{R}_1$ and $\boldsymbol{R}_2$ are positive semi-definite weighting matrices, which are used for tuning. With

$$\boldsymbol{R}_2 = \begin{cases} \boldsymbol{R}_{21} & \text{if } \vartheta_{\text{ICB}} \geq \vartheta_{\text{ICB}}^{\text{ref}} \\ \boldsymbol{R}_{22} & \text{if } \vartheta_{\text{ICB}} < \vartheta_{\text{ICB}}^{\text{ref}} \end{cases}$$

and

$$\boldsymbol{R}_1 = R_1\boldsymbol{I}, \quad \boldsymbol{R}_{21} = R_{21}\boldsymbol{I}, \quad \boldsymbol{R}_{22} = R_{22}\boldsymbol{I},$$

where $\boldsymbol{I} \in \mathbb{R}^{(N_c \times N_c)}$ is the identity matrix, the penalty of the output can defined for different directions of the deviation separately, see Fig. 5. The weighting matrices R_{21} and R_{22} depend on $\vartheta_{\text{ICB}}^{\text{ref}}$ (whether its smaller or greater than 0°C) and the distance between $\vartheta_{\text{ICB}}^{\text{ref}}$ and zero. The weighting matrix which penalises the region between $\vartheta_{\text{ICB}}^{\text{ref}}$ and zero is much larger to avoid unfreezing/freezing.

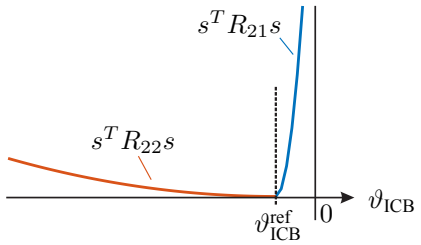

Fig. 5 Output constraint with different weighting matrices R_{21} and R_{22} for $\vartheta_{\text{ICB}}^{\text{ref}} < 0$.

The corresponding optimisation problem is formally stated as

$$J^\star = \min_{\boldsymbol{U}} J, \tag{14}$$

and the optimal control values $\dot{Q}_0^\star$ are given by

$$\dot{Q}_0^\star = \arg\min_{\boldsymbol{U}} J, \tag{15}$$

which is the desired input for the optimal rotational speed of the RS.

4. SIMULATION RESULTS

The simulation setup is given by consecutive door-openings of a cooled ICB which causes a step-wise decrease of cargo mass. Unloading times and durations are assumed to be a priori known, this knowledge coming from a pre-planned route and real-time geographic information. The interval of the door-opening is defined by t_{period} and the door-opening duration is defined by t_{door}.

A comparison with a state-of-the-art PI-control is given, and the MPC behaviour with and without output constraints is analysed.

4.1. Parameters

The values for mass, heat capacities and heat transfer coefficients result as follows:

$$\boldsymbol{m} = \begin{bmatrix} 1000 \\ 4.29 \\ 94.95 \\ 10.87 \\ 10.87 \\ 10.87 \\ 10.87 \\ 10.87 \\ 237.37 \end{bmatrix}, \quad \boldsymbol{cp} = \begin{bmatrix} 3000 \\ 1006 \\ 460 \\ 1300 \\ 1300 \\ 1300 \\ 1300 \\ 1300 \\ 460 \end{bmatrix}, \quad \boldsymbol{\alpha} = \begin{bmatrix} 10 \\ 20 \\ 6.67 \\ 3.34 \\ 3.34 \\ 3.34 \\ 3.34 \\ 6.67 \\ 19.99 \end{bmatrix},$$

where five insulation layers of the PU elements ($n_{\text{PU}} = 5$) are used. In Table 1 the parameters of the model are shown. All control parameters are shown in Table 2.

Parameter	Value	Parameter	Value
ϑ_{amb}	35°C	$\vartheta_{\text{ICB}}^{\text{ref}}$	-10°C
A_{iso}	15.1 m^2	A_{cargo}	4.56 m^2
t_{period}	900 sec	t_{door}	120 sec
$m_2(0)$	500 kg	d_{cargo}	50 kg

Table 1 Model parameters. The cargo mass on the beginning of the simulation is denoted by $m_2(0)$.

Table 2.

Parameter	Value	Parameter	Value
T_s	1	N_p	300
R_1	1	N_c	250
R_{21} (small)	10e+7	K_P	-4950
R_{21} (large)	10e+12	K_I	-1.6639e+04
R_{22}	10e+3		

Table 2 Control parameters.

The MPC with its constraint quadratic programming problem is solved with the *quadprog* algorithm.

4.2. PI-controller vs MPC

The MPC is compared to an industry standard PI-controller. In Fig. 6 the solution is plotted over 4.17 h. The door-opening impact is shown in Fig. 3, (blue line). It can be seen that due to the output constraint the MPC can hold the temperature below $0°C$. It can also be seen that due to the air mass change the ICB temperature is the most critical temperature and the door-opening does not have a significant impact on the outer insulation layers.

In Fig. 7 the heat impact of the door-opening (blue) and the decreasing cargo mass (red) is shown.

In Fig. 8 the cooling capacity and temperature of the ICB is plotted over 0.3 h. Two MPCs with different weighting matrices R_{21} and the PI controller are compared. The MPC ($\text{MPC}_{\text{R,large}}$) plotted in red has a greater R_{21} than the MPC ($\text{MPC}_{\text{R,small}}$) plotted in blue. Therefore, the temperature near to zero is more penalised, which means that the controller has to cool down the ICB

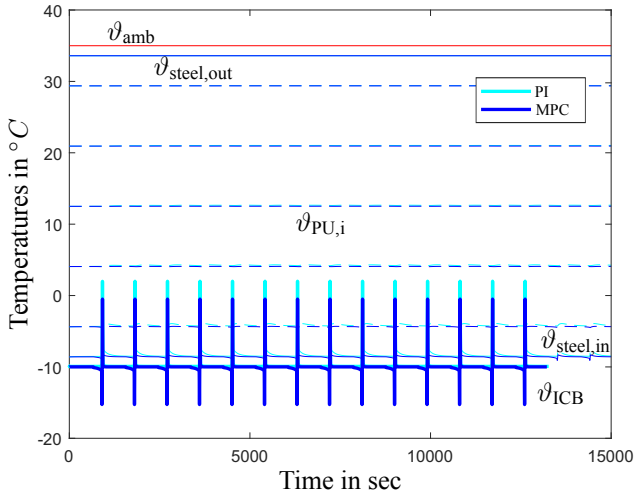

Fig. 6 All temperatures over time with door-opening. The result of the MPC (blue lines) is compared with the PI controller (cyan lines).

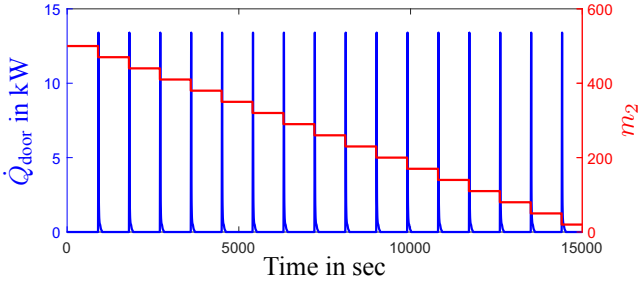

Fig. 7 Heat flow of door-opening and mass decreasing over time.

before the door is opened. It can be seen that the PI controller is not able to hold the temperature in the negative region (cyan line).

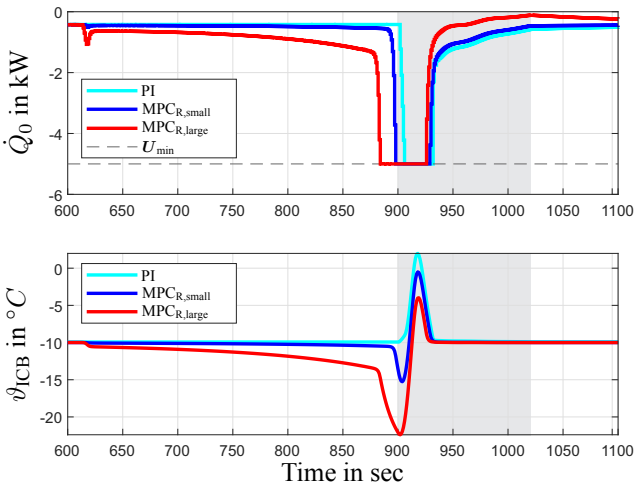

Fig. 8 Cooling capacity and ICB temperature during one door-opening interval (grey).

In Fig. 9 the cumulative sum of the cooling capacity is shown. It can be seen that the MPC (blue line) needs less cooling capacity to ensure the output constraint. Depending on the weighting matrices of the output constraint the necessary cooling capacity has to increase (red line).

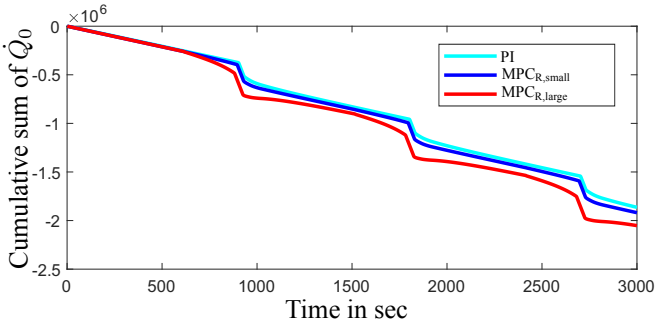

Fig. 9 Cumulative sum of the cooling capacity for three door-openings.

4.3. Constrained MPC

In Section 4.2 results have been shown where cooling during door-opening is allowed. Due to the open door cooling is not energy efficient. Therefore, in this Section the MPC includes hard input constraints which ensures that the RS is not used during door-opening

$$\boldsymbol{U}_{\min} = \mathbf{0} \quad \text{if} \quad \dot{\boldsymbol{Q}}_{\text{door}}^{\text{traj}} > 0. \tag{16}$$

In Fig. 10 the results with such a constraint, eq. (16) is shown. Two MPCs are compared, the first without the output soft constraints ($MPC_{Y,unconstr}$) and the second where the output soft constraints are active ($MPC_{Y,constr}$). It can be seen that with active output constraints the controller is able to hold the temperature in the allowed temperature region, but in order to achieve this a strong reduction of the ICB air temperature at an early stage is necessary. The results depend strongly on the prediction and control horizon of the MPC.

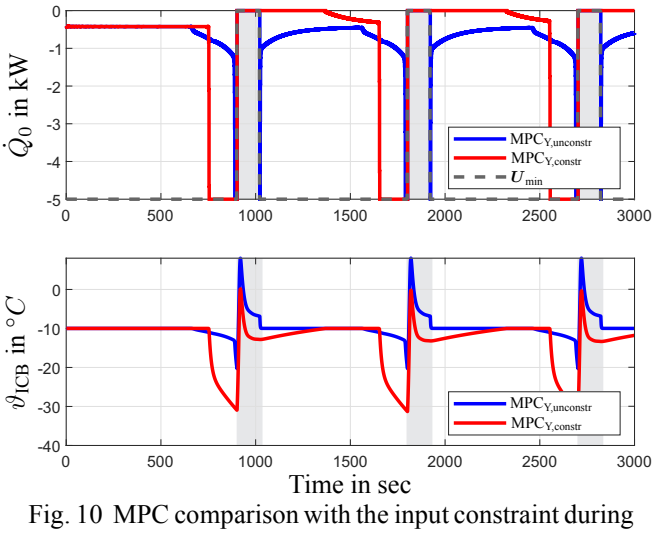

Fig. 10 MPC comparison with the input constraint during door-opening with the door-opening interval (grey).

In Fig. 11 the cumulative sum of the cooling capacities of the simulation in Fig. 10 is shown.

In Table 3 the control concepts are compared. The first column shows the cooling energy E for the simulation normalised with the value of the PI controller. The second column shows the maximal ICB temperature value.

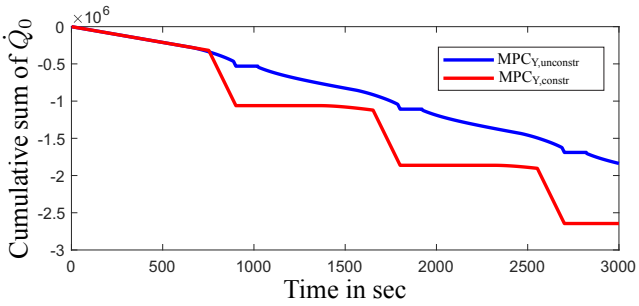

Fig. 11 Cumulative sum of the cooling capacity.

Method	Fig.	E	ϑ_{ICB}^{max} in °C
PI	8	1	2⋆
MPC$_{R,small}$	8	1.03	-0.5
MPC$_{R,large}$	8	1.10	-3.98
MPC$_{Y,unconstr}$	10	0.99	8.02⋆
MPC$_{Y,constr}$	10	1.42	0

Table 3 Control performance comparison (⋆violation of negative ICB temperature).

4.4. Control of the cargo temperature

Controlling the cargo temperature has benefits to the RS.

In Fig. 12 the temperatures over one door-opening are shown.

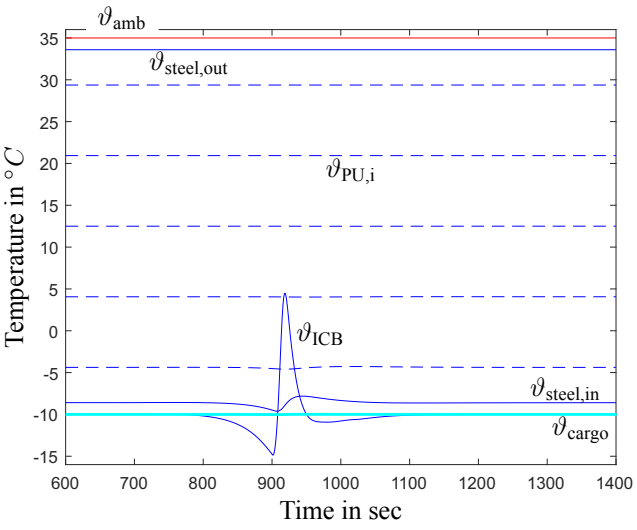

Fig. 12 All temperatures during one door-opening where the cargo temperature is controlled.

In Fig 13 the deviation of the cargo temperature during a door-opening is shown. It can be seen that it is possible to control the cargo temperature in such a small region which is even not measurable by a standard sensor. The temperature of the cargo stays in a region of $\pm 0.02°C$. Due to the thermal inertia of the cooled goods, no additional cooling capacity would be necessary during door-opening.

5. DISCUSSION

A massive heat loss during door-opening is inevitable. Nevertheless, a suitable control strategy can guarantee

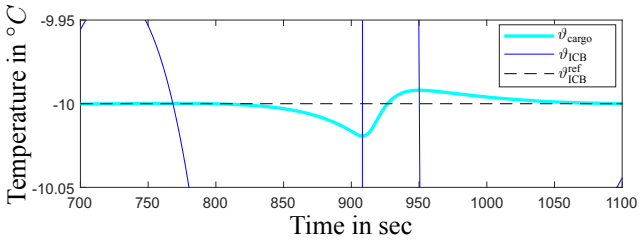

Fig. 13 Zoom in of the cargo temperature.

compliance with temperature limits and minimise energy consumption. As shown in Table 3 these two goals are in principle conflicting, and MPC cannot overcome this fact. However, the added flexibility of the MPC (especially constraint handling) is an important feature for temperature control during door-opening; additionally, the energy consumption for a given performance is also minimised.

Stability of the proposed control concept is guaranteed if the model is correct and feasibility of the MPC optimization is given. Note that the soft constraint for the output ensures feasible solutions in all situations. The numerical effort for solving the optimization for one control input with one hard constraint and the given prediction and control horizons, respectively, is acceptable. Due to the fast dynamics of the ICB air temperature during door opening a small sampling interval is necessary, however, due to the comparatively small cooling capacity of the ICB long horizons are necessary. If control of the cargo temperature could be used the sampling time could be increased and, therefore, the computational cost could be further decreased (e.g. $T_S = 10$ sec, $N_p = 30$ and $N_c = 25$).

Direct control of the cargo temperature is obviously an attractive approach. The main problem is posed by a reliable measurement of the cargo temperature. Future regulations could provide wireless temperature probes inside the transported goods, thus delivering direct measurement of the cargo temperature. Current investigations evaluate information from miniature infrared cameras to obtain surface temperatures of the cargo. This is, however, an indirect measurement, and the estimation of the true cargo temperature still relies on a accurate model of package and cargo. For controlling both temperatures with strongly differing different time constants a controller with multi-rate sampling can be used, [3].

6. CONCLUSION

In this paper the temperature control of a food transport system with an insulated cool box (ICB) by model predictive control is presented. The proposed control scheme explicitly covers door-opening which is the reason for a large part of total cooling load.

Simulation results show that the performance can be improved compared to a standard PI controller. With output constraints the MPC is able to handle the door-opening without violating the allowed temperature region of the ICB air temperature. Nevertheless, high cooling capacity is necessary. The simulation results also show

that controlling the cargo temperature instead of the ICB air temperature would be an important factor for reduction of energy consumption.

ACKNOWLEDGEMENTS

The authors wish to thank PRODUCTBLOKS GmbH in Korneuburg, Austria. This work was supported by the project ”CONSERVE” (FFG, No. 21860205).

REFERENCES

[1] S. James, C. James, J. Evans, Modelling of food transportation systems–a review, International Journal of Refrigeration 29 (6) (2006) 947–957.

[2] E. Luchini, A. Schirrer, M. Kozek, A hierarchical mpc for multi-objective mixed-integer optimisation applied to redundant refrigeration circuits, IFAC-PapersOnLine 50 (1) (2017) 9058–9064.

[3] E. Luchini, A. Schirrer, S. Jakubek, M. Kozek, Model predictive multirate control for mixed-integer optimisation of redundant refrigeration circuits, Journal of Process Control 76 (2019) 112–121.

[4] E. Luchini, M. Kozek, Disturbance observer and ageing estimation for a temperature controlled food transporter, in: 2018 SICE International Symposium on Control Systems (SICE ISCS), IEEE, 2018, pp. 97–104.

[5] E. Luchini, D. Radler, D. Ritzberger, S. Jakubek, M. Kozek, Model predictive temperature control and ageing estimation for an insulated cool box, Applied Thermal Engineering 144 (2018) 269–277.

[6] P. Chen, D. Cleland, S. Lovatt, M. Bassett, An empirical model for predicting air infiltration into refrigerated stores through doors, International Journal of refrigeration 25 (6) (2002) 799–812.

[7] A. Foster, R. Barrett, S. James, M. Swain, Measurement and prediction of air movement through doorways in refrigerated rooms, International journal of refrigeration 25 (8) (2002) 1102–1109.

[8] T. L. de Micheaux, M. Ducoulombier, J. Moureh, V. Sartre, J. Bonjour, Experimental and numerical investigation of the infiltration heat load during the opening of a refrigerated truck body, International Journal of Refrigeration 54 (2015) 170–189.

[9] S. Tian, Y. Gao, S. Shao, H. Xu, C. Tian, Numerical investigation on the buoyancy-driven infiltration airflow through the opening of the cold store, Applied Thermal Engineering 121 (2017) 701–711.

[10] S. Tian, Y. Gao, S. Shao, H. Xu, C. Tian, Measuring the transient airflow rates of the infiltration through the doorway of the cold store by using a local air velocity linear fitting method, Applied Energy 227 (2018) 480–487.

[11] S. Tian, Y. Gao, S. Shao, H. Xu, C. Tian, Development of an unsteady analytical model for predicting infiltration flow rate through the doorway of refrigerated rooms, Applied Thermal Engineering 129 (2018) 179–186.

[12] G. Bejarano, J. A. Alfaya, M. G. Ortega, M. Vargas, On the difficulty of globally optimally controlling refrigeration systems, Applied Thermal Engineering 111 (2017) 1143–1157.

[13] G. Bejarano, C. Vivas, M. G. Ortega, M. Vargas, Suboptimal hierarchical control strategy to improve energy efficiency of vapour-compression refrigeration systems, Applied Thermal Engineering 125 (2017) 165–184.

[14] E. F. Camacho, C. B. Alba, Model predictive control, Springer Science & Business Media, 2013.

[15] L. Wang, Model predictive control system design and implementation using MATLAB, Springer Science & Business Media, 2009.